Published in final edited form as:
Neurobiol Dis. 2008 November ; 32(2): 229–242. doi:10.1016/j.nbd.2008.06.018.

The Synaptic Impact of the Host Immune Response in a Parkinsonian Allograft Rat Model: Influence on Graft-Derived Aberrant Behaviors

KE Soderstrom[1], **G Meredith**[2], **TB Freeman**[3], **SO McGuire**[4], **TJ Collier**[5], **CE Sortwell**[5], **Qun Wu**[6], and **K Steece-Collier**[5]

KE Soderstrom: katherinesoderstrom@yahoo.com; G Meredith: gloria.meredith@rosalindfranklin.edu; TB Freeman: tfreeman@health.usf.edu; SO McGuire: smcguire@lumc.edu; TJ Collier: timothy.collier@uc.edu; CE Sortwell: caryl.sortwell@uc.edu; Qun Wu: qunpdwu@hotmail.com; K Steece-Collier: kathy.collier@uc.edu

[1] Department of Neurological Sciences, Rush University, Chicago, IL

[2] Department of Cellular and Molecular Pharmacology, Rosalind Franklin University, North Chicago, IL

[3] Department of Neurosurgery, University of South Florida, Tampa, FL

[4] Department of Pathology, Loyola University Medical School, Loyola University Chicago, Maywood, IL

[5] Department of Neurology, University of Cincinnati, Cincinnati, OH

[6] Department of Psychiatry, Maine Medical Center, Portland, MA

Abstract

Graft-induced dyskinesias (GIDs), side-effects found in clinical grafting trials for Parkinson's disease (PD), may be associated with the withdrawal of immunosuppression. The goal of this study was to determine the role of the immune response in GIDs. We examined levodopa-induced dyskinesias (LIDs), GIDs-like behaviors, and synaptic ultrastructure in levodopa-treated, grafted, parkinsonian rats with mild (sham), moderate (allografts) or high (allografts plus peripheral spleen cell injections) immune activation. Grafts attenuated amphetamine-induced rotations and LIDs, but two abnormal motor syndromes (tapping stereotypy, litter retrieval/chewing) emerged and increased with escalating immune activation. Immunohistochemical analyses confirmed immune activation and graft survival. Ultrastructural analyses showed increases in tyrosine hydroxylase-positive (TH+) axo-dendritic synapses, TH+ asymmetric specializations, and non-TH+ perforated synapses in grafted, compared to intact, striata. These features were exacerbated in rats with the highest immune activation and correlated statistically with GIDs-like behaviors, suggesting immune-mediated aberrant synaptology may contribute to graft-induced aberrant behaviors.

Keywords

Grafting; Parkinson's disease; Ultrastructure; Immunology; Dopamine; Synaptic Plasticity

Address correspondence to: Kathy Steece-Collier, Ph.D. Department of Neurology, University of Cincinnati, Cincinnati OH, 45267, Phone: 513.558.1167, Fax: 513.558.2965, kathy.collier@uc.edu.

Introduction

A major set-back to embryonic dopaminergic grafting trials in Parkinson's disease (PD) patients has been the development of troublesome post-graft abnormal involuntary movements in as many as 50% of trial participants (Hagell et al., 2002; Olanow et al., 2003). These so-called graft-induced dyskinesias (GIDs) have characteristics largely unique from common levodopa-induced dyskinesias (LIDs) and appear to more closely resemble biphasic drug-induced dyskinesias (Cenci and Hagell, 2005), often involving stereotypy and hyperkinesia and localized to either upper or lower extremities (Olanow et al., 2003; Hagell et al., 2002). This is in contrast to peak-dose LIDs, which are more widespread (involving both pair of extremities) and primarily dystonic and choreic (Fahn et al., 2000). Unlike peak dose LIDs, GIDs are most commonly noted when plasma levodopa levels are low. An animal model of GIDs has recently been reported (Steece-Collier et al., 2003; Maries et al., 2006; Lane et al., 2006; Carlsson et al., 2006). While differences exist between clinical GIDs and the rat model, in both humans (Freed et al., 2001; Hagell et al., 2002; Olanow et al., 2003) and animals (Maries et al., 2006), grafting embryonic dopaminergic neurons into the parkinsonian striatum can result in the development of novel, aberrant motor behaviors at extended post-graft intervals.

Clinical observations suggest a link between the host immune system and GIDs. Specifically, GIDs were reported in patients that received no immunsuppression (Freed et al., 2001) or soon after the withdrawal of immunosuppression (Olanow et al., 2003; Hagell and Cenci, 2005). In two patients displaying GIDs, post-mortem examination showed that the surviving grafts were surrounded by activated microglia (Olanow et al., 2003). This coincidence of GIDs development and immunosuppression withdrawal suggests the host immune response contributes to the development of these behaviors following dopaminergic grafting in the parkinsonian brain; however, this hypothesis remains to be tested.

An immune-mediated alteration in synapses is a possible explanation for the emergence of GIDs (e.g.: Tonelli et al., 2005). Indeed, synaptic remodeling is a key feature of neuroleptic-induced dyskinesias (Meredith et al., 2000), indicating a direct link between synaptic structural changes and dyskinesias. The dendrites of medium spiny neurons (MSNs) are densely covered with spines, which are the primary targets of afferent, cortical glutamatergic and nigral dopaminergic neurons (Bolam, 1984; Freund et al., 1984). There is evidence from earlier studies that striatal dopaminergic grafts that reinnervate the host form aberrant connections with these MSNs (Freund et al., 1985; Mahalik et al., 1985; Clarke et al., 1988; Leranth et al., 1998). However, none of these studies examined the potential importance of these or other synaptic changes in the graft-host relationship over time, or in the emergence of abnormal behaviors.

We examined varying levels of immune activation on striatal synaptic organization in a well-characterized rat allograft model (Duan et al., 1995a; 1995b; 1997), as a first step in understanding whether immune cells impact the ultrastructural characteristics of new synapses from grafts or existing host terminals. We then correlated changes in the synaptic organization with GIDs in these rats.

MATERIALS & METHODS

Animals

Adult male Sprague Dawley rats (225–250g at the start of the study) were kept on a 12-hour light-dark cycle with *ad libitum* food and water. The rats were housed and treated according to the rules and regulations of NIH and Institutional Guidelines on the Care and Use of Animals. To correlate host immune response severity with the severity and frequency of dyskinesias,

rats were placed into 1 of 3 groups of varying immune status: 1) minimal immune response (sham-grafted rats; n=16), 2) moderate immune response (rats receiving allografts and sacrificed at 21 weeks post-grafting; “G21”; n=8), and 3) high immune response (allografted rats receiving secondary immune challenges with peripheral spleen cell injections on weeks 10 and 18 post-grafting; “G21 + spleen”; n=9). All rats in groups 1–3 were sacrificed at 21 weeks post-grafting. A fourth group of allografted rats was sacrificed at 10 weeks post-grafting (“G10”; n=10) to provide baseline information for this earlier post-graft time-point, prior to any spleen cell injections. Additionally, behavior from a previously studied group displaying a mild immune response was also analyzed (syngeneic-grafted rats where donor and host were of the same strain (Fisher 344), had identical experimental lesion and graft parameters, and were sacrificed on week 10 post-grafting; n=10). The groups and the timeline of surgeries and treatments are shown in Figure 1.

Nigrostriatal lesions

Rats were anesthetized with a chloropent solution and secured in a stereotaxic apparatus. Two μl of 6-hydroxydopamine (6-OHDA; 6μg free base/3μl 0.02% ascorbate made in sterile saline) was injected at a flow rate of 1μl/min using a Hamilton 26 gauge needle to 2 sites unilaterally (to the medial forebrain bundle; A/P= 4.8mm, M/L= 1.7mm from bregma, D/V= 7.5mm from dura, and substantia nigra; A/P= 4.3, M/L= 1.2mm from bregma, D/V= 7.5mm from dura).

Amphetamine-induced rotational behavior

For behavioral assessment of lesion success and graft efficacy, amphetamine-induced rotational analyses were performed on week -4 (2 weeks following lesion, 4 weeks prior to neural grafting), and weeks 9, 16 and 20 post-grafting. Rats received intraperitoneal injections of amphetamine sulfate (5mg/kg) and rotational behavior was quantified for 90 minutes post-injection using automated rotometers. Rats that displayed more than 7 turns per minute were determined to have sustained approximately 90% nigral dopaminergic cell loss and were included in the study.

Levodopa treatment

To induce LIDs, 2 weeks post-lesion, rats received intraperitoneal injections of levodopa and the peripheral decarboxylase inhibitor, benserazide (one week of 25mg/kg levodopa; 25mg/kg benserazide followed by three weeks of 12.5mg/kg levodopa; 12.5mg/kg benserazide) in sterile injection saline daily at approximately the same time of the day (Monday-Friday). Following grafting, levodopa was withheld for 7 days to prevent any potential toxic effects to grafted cells by levodopa. Following this “drug holiday”, rats resumed daily treatments (5 days per week; 12.5mg/kg levodopa; 12.5mg/kg benserazide) for the duration of the study.

Fetal mesencephalic allograft preparation

Embryonic cells of the ventral mesencephalon were obtained from embryonic day 14 (crown-rump length of 10.5 to 11.5 mm) Lewis rats for allografts using micro-dissection techniques and tissue was prepared as previously described (Maries et al., 2006). Final suspensions for transplantation were prepared at an approximate density of 125,000 cells/μl Neurobasal media (Invitrogen).

Fetal mesencephalic allograft injections

Rats were anesthetized with a chloropent solution and secured in a stereotaxic apparatus. Two μl of cell suspension (~250,000 cells total per site) were injected into 2 sites in the striatum (site 1: A/P= 1.6, M/L= 3.2 from bregma, D/V= 4.5 from dura; site 2: A/P= 0.5, M/L= 3.5 from bregma, D/V= 4.5 from dura) at flow rate of 0.5μl/minute using a Hamilton 26 gauge needle.

Sham-grafted rats received equal volumes of the cell-free suspension media. For all grafts, the needle was left in place for 3 minutes following deposition of tissue or vehicle.

Dyskinesia rating

Abnormal involuntary movements or posturing associated with levodopa or graft treatment, are referred to in this text as dyskinesias. Dyskinesias observed in levodopa-treated parkinsonian rats included dystonic and hyperkinetic behaviors. Dystonic behaviors were characterized by abnormal muscle tone, which was noted as excessive stiffness and rigidity, and/or abnormal posturing of the neck, trunk, right forepaw and/or right hindpaw. Hyperkinetic dyskinesias consisted of vacuous chewing and/or protrusion of the tongue (orolingual), repetitive, rhythmic bobbing of the head and neck (head-bob) and stereotypic and/or chorea-like movements of the right forepaw (right forepaw dyskinesia: RFPD). Dyskinetic behaviors were scored by an observer blinded to treatment group 3 days per week, Wednesday through Friday. Each rat was observed for 2 minutes precisely 30 minutes following levodopa treatment.

A cumulative score for total LIDs was obtained through the summation of the frequency (0–3, with 0= no expression, 1= expression less than 50% of the time, 2= expression more than 50% of the time and 3= constant expression) and the intensity (0–3, with 0= no expression, 1= mild expression, 2= moderate expression, 3= severe expression) of the individual scores. Additionally, rats were rated for novel dyskinetic behaviors that emerged with graft maturation. These included two similar but distinct behaviors involving orolingual and contralateral forelimb behaviors. The first was a compulsive tapping or pushing of cage litter with the forelimb contralateral to the graft (tapping dyskinesia), and a second was a ‘goal directed’, stereotypic retrieving of litter with the forepaw contralateral to graft and/or chewing of the litter, termed here as facial forelimb dyskinesia. A cumulative score for total GIDs-like behaviors was obtained with the same frequency rating, but intensity was rated as either absent (score= 0) or present (score= 1).

For all behaviors observed, the intensity and the frequency were quantified simultaneously. The product of the intensity and frequency scores provided a final “severity” score, which was obtained daily for each behavior and averaged to provide a weekly score. A detailed description of this rating scale is reported elsewhere (Steece-Collier et al., 2003; Maries et al., 2006).

Peripheral spleen cell injections

The delivery of peripheral immunogeneic spleen cell injections has been shown to exacerbate immune activation in allografted rats (e.g.: Duan et al., 1997). In order to enhance the host immune response in a subset of allografted rats in our study, designated subjects received a subcutaneous injection of Lewis rat donor-derived spleen cells (1,000,000 total cells per injection; 25,000/μl). Spleen cells were administered at week 10, and again at week 18, post-grafting.

Tyrosine hydroxylase immunohistochemistry

Rats used for the evaluation of immunohistochemistry were sacrificed 21 weeks post-grafting by transcardial perfusion with 0.9% saline followed by cold 4% paraformaldehyde, pH 7.6 at 4°C. The brains were removed, post-fixed in paraformaldehyde for 24 hours, followed by immersion in 30% sucrose solution until saturated. Brains were sectioned in the coronal plane on a freezing microtome into sections 35 μm thick. Brains were serially sectioned into 6 sets per brain and stored at −20°C in cryoprotective solution until ready for analysis.

Every sixth coronal section was stained with antisera against tyrosine hydroxylase (TH) to visualize grafted dopaminergic cells. Sections were incubated overnight at room temperature

(RT) in 1:4000 monoclonal anti-TH primary antibodies (Chemicon Inc., CA). The following day sections were rinsed and then incubated for 2.5 hours in 1:400 goat anti-mouse IgG biotinylated secondary antibody (Vector Laboratories, Burlingame, CA) and developed using 0.05% 3,3-diaminobenzidine tetrahydrochloride (DAB) and 0.01% hydrogen peroxide.

To analyze graft survival, a total of 3 equally spaced TH-immunopositive (TH+) sections were analyzed for each graft injection. Each was outlined at a magnification of 4× and TH+ cells were counted at 60× with oil immersion. Each section was overlaid with a grid and cells were counted in equally spaced counting frames using dedicated software (MicroBrightField Williston, VT). A total number of grafted neurons was estimated from this semi-quantitative method.

MHC class II immunohistochemistry

Every sixth striatal section was immunoreacted with antisera against the major histocompatability (MHC) class II molecule to visualize antigen-presenting cells as a measure of immune activation. Sections were incubated overnight at RT in 1:500 monoclonal mouse anti-MHC class II primary antisera (Serotec, Raleigh, NC). The following day sections were rinsed and then incubated for 2.5 hours in 1:1000 biotinylated goat anti-mouse secondary antibody (Vector Laboratories, Burlingame, CA) and avidin biotin complex (ABC Kit, Vector Laboratories, Burlingame, CA) and developed using DAB.

Stereology

To analyze the host immune response, MHC class II+ cells were counted using unbiased stereology with the optical fractionator method (Gundersen, 1986). After a random start, every sixth section was selected for analysis for each rat. Anatomical boundaries for the striatum were delineated with the aid of an atlas (Paxinos) and included only the dorsal striatum. The entire rostral caudal extent of the striatum was analyzed with hardware and software dedicated to stereology (StereoInvestigator, MicroBrightField Williston, VT). A systematic random sample of cells was achieved by positioning a sampling grid over the striatum on each of the selected sections. The grid was divided into counting frames of 50 × 50 μm that were equidistant from one another. Their number was established so that no more than 200 cells were counted for each rat. Optical disector counting rules were applied to estimate the total number of cells in each disector volume. The volume of the striatum was calculated following the rules of Cavalieri.

Electron microscopy (EM)

Allografted rats used for ultrastructural analyses were sacrificed at weeks 10 (baseline) or 21, post-grafting, by transcardial perfusion with 0.1M phosphate-buffered saline (0.1M PBS) followed by 4% paraformaldehyde and 0.1% glutaraldehyde in PB. Brains were post-fixed for 2 hours at 4°C in the same fixative without glutaraldehyde. Brains were washed thoroughly in PB, and sections were cut in the horizontal plane at 60μm thickness on a Vibratome (The Vibratome Company, St. Louis, MO).

TH immunohistochemistry for EM

Sections were collected in 0.1M PB and alternate sections of the striatum from the intact and dopamine-depleted hemispheres were submitted to a “freeze-thaw” regimen (Meredith et al., 2000) before incubation with antisera against TH (1:2000; Immunostar, Hudson, WI) for 16–20 h at 4°C. Sections were then rinsed and incubated in biotinylated goat anti-mouse IgG (Vector Laboratories, Cupertino, CA) for 2 hours at RT and then placed in ABC (Elite kit, Vector Laboratories) according to the manufacturer’s instructions. Sections were then rinsed and reacted with DAB. They were then flattened onto glass slides and covered with 1% osmium

tetroxide (in 0.1% cacodylate buffer, pH 6.8) for 45 min, dehydrated through a graded ethanol series, including 40 minutes in a saturated solution of uranyl acetate in 70% ethanol, and embedded in resin (EMBED-812, Electron Microscopy Sciences, Ft. Washington, PA).

Ultrastructural analysis

Sections were flat mounted between 2 rectangular sheets of ACLAR plastic onto a glass slide. Small weights compressed the section "sandwich" during curing in a 60ºC oven for 3 days. Sections were viewed under a dissection microscope and the outline of the striatum was drawn and graft locations were marked. The top plastic layer was removed and 2–4 small pieces of tissue from the striatum were excised and mounted onto pre-formed resin blocks using fresh resin. These blocks were then re-sectioned using an ultramicrotome (Ultracut E, Leica, Wetzler, Germany) at 60–70 nm (silver) and serial sections were collected onto slot, pioloform-coated, copper grids. The sections were contrasted with 1% lead citrate and examined in a JEOL 1230 JEM electron microscope. Blocks were taken from 2 horizontal sections of the dopamine-depleted grafted or intact striata, of 14 animals (4–5 rats/group). Images of TH+ and unstained asymmetric synapses were digitally captured (Multiscan, Gatan, Warrendale, PA) at 80kV and 25,000× and again at 60,000× for analysis. Micrographs were created from files imported as TIFFs into Adobe Photoshop, adjusted for contrast, re-sized, and assembled into plates.

Synapses were identified on the basis of the presence of vesicles in the presynaptic bouton close to the cleft, and thickened, parallel membranes (active zone). Postsynaptic structures and specializations were identified according to descriptions in Peters et al. (1991). Each perikaryon had an identifiable nucleus and cytoplasm with typical organelles. Dendrites had smooth contours and contained mitochondria, microtubules and rough endoplasmic reticulum. Spines were small structures identified by a spine apparatus, when visible in the plane of section. However, if the apparatus was not apparent, small structures were classified as spines if they lacked the organelles found in dendrites and contained an easily identified, unlabeled asymmetric input. Synapses were identified as asymmetric if the postsynaptic density was 2.5–3 times the width of the presynaptic density (Groves et al., 1980). For the data presented, approximately 10,000μm^2 of tissue was examined.

Statistics

Pooled time series analysis was used for dyskinetic behaviors that had extensive temporal data. This approach improves statistical efficiency for estimates of the populations being studied over prolonged periods of time. Briefly, the number of time-points analyzed was reduced through the averaging of non-significantly different time-points within groups as determined by one-way analyses of variance (ANOVAs). The results of these groupings were a "pre-graft maturation" time-point (the average of weeks −3 to −1 pre-grafting and week 2 post-grafting), an "early post-grafting" time-point (the average of weeks 4, 6, 8 and 10 post-grafting), a "mid post-grafting" time-point (the average of weeks 12, 14, 15, 16, 17 post-grafting) and a "late post-grafting" time-point (the average of weeks 18, 19, 20 and 21 post-grafting).

A two-way repeated measures ANOVA was performed for each behavior, to assess the effects of treatment, time, and treatment by time interaction. Significant differences of main effects were determined using Bonferroni post-hoc analyses. On significant time-points of interest (weeks 2, 4, 10 and 18 post-grafting) one-way ANOVAs were performed to determine any effect of group for each behavior analyzed. Significant differences between groups were determined using Tukey's post-hoc analyses.

Differences in TH+ and MHC class II+ cell counts were determined using Student t-test analyses and one-way ANOVAs followed by Tukey's post-hoc analyses. Differences in active zone lengths were determined using a one-way ANOVA followed by Newman-Keuls post-hoc

analyses. Differences in postsynaptic targets and synaptic specializations were determined using Chi Square (χ^2) analyses at a level of significance at p= 0.05, two-tailed. Correlations between ultrastructural, immunohistochemical and behavioral analyses were performed using Spearman correlation tests.

Results

Behavioral analysis

Amphetamine-induced rotational behavior—Rats were observed 2 weeks following 6-OHDA and again on weeks 9, 16 and 20 post-grafting to determine lesion success and post-graft behavioral recovery. Two weeks post-lesion (pre-graft), rats in all groups showed a similar severity in amphetamine-induced contralateral turns per 90 minutes ($F^{2,30}$= 0.62, p= 0.55; Sham: 852.88 ± 87.47; Allograft: 714.50 ± 67.85; G21 Allograft + spleen: 841.33 ± 88.90). However, by week 9 post-grafting, all dopamine-grafted groups showed significant improvements compared to sham groups ($F^{2,30}$= 21.25, p< 0.001; Sham: 871.63 ± 121.44; Allograft: 16.25 ± 187.83; Allograft + spleen: −245.56 ± 77.88) that were sustained throughout the experiment (week 20 post-grafting: $F^{2,30}$= 13.89, p< 0.001; Sham: 836.44 ± 107.86; Allograft: −73.25 ± 225.03; Allograft + spleen: −111.89 ± 169.96) and were not altered by the delivery of a secondary immune challenge (Allograft vs. Allograft + spleen: p= 0.99).

Levodopa-induced dyskinesias—Dyskinetic posturing and movements were observed at time-points prior to and following grafting to determine the effects of grafting and immune status on classic LIDs (i.e., those noted prior to grafting or in non-grafted rats). Four weeks following the delivery of embryonic grafts to the dopamine-depleted striatum all dopamine-grafted rats showed a significant attenuation of total LIDs relative to rats receiving sham grafts (week 4 post-grafting: $F^{2,30}$= 8.81; Fig 2A). While all allografted rats showed a stable significant reduction in these LIDs-like behaviors post-grafting, allograft + spleen rats showed an additional transient trend towards further reduction following the second spleen cell injection when compared to sham rats (week 18 post-grafting: $F^{2,30}$= 13.41; Fig 2A).

Graft-induced dyskinesias—Rats were observed prior to and following grafting to examine the impact of implantation of embryonic dopaminergic neurons into the parkinsonian striatum and the level of host immune response on the development of novel aberrant behaviors. All allografted Sprague Dawley rats receiving tissue from Lewis donors developed significant levels of two novel abnormal motor stereotypies - contralateral forelimb tapping dyskinesia and forelimb-facial dyskinesia - in the weeks following grafting. As we have reported previously (Maries et al., 2006), maturation of grafted dopaminergic neurons in parkinsonian rats is associated with the attenuation of LIDs, and the emergence of these graft-associated aberrant behaviors. In the current study, the severity of total GIDs behavior (tapping dyskinesia + forelimb facial dyskinesia) in all allografted rats was noted to develop to significant levels compared to sham rats at week 4 post-grafting ($F^{2,30}$= 12.11; Fig 2B). These graft-related aberrant behaviors were distinct from typical pre-graft LIDs behavior in both form and time course, and were characterized by their focal (localized to the forepaw contralateral to the graft and/or face) and stereotypic manifestation. In all allografted rats, these behaviors occurred following dopaminergic neuron transplantation and were never seen prior to grafting.

To determine whether these post-graft aberrant motor behaviors were affected by host immune status, the severity of these behaviors was compared between sham-grafted (low-to-no immune response), allografted rats (G21; moderate immune response) and allografted rats plus secondary spleen challenge (G21 + spleen; high immune response). Statistical analyses determined that there was a significant, but transient enhancement of tapping dyskinesia behavior following spleen cell delivery in rats receiving a secondary immune response

compared to G21 alone rats (week 10: $F^{2,30}$= 18.34; week 18: $F^{2,30}$= 12.11; Fig 2C). There was no overall significant difference in the severity of forelimb facial dyskinesia between G21 and G21 + spleen rats. Further, it is noteworthy that these aberrant post-graft motor behaviors failed to show significant development in syngeneic-grafted rats run in tandem with the current allogeneic rats under an identical grafting paradigm, but sacrificed for a separate experiment (Fig 2D).

Dopaminergic grafts and the host immune response

Dopaminergic grafts: gross and ultrastructure evaluations—Grafted neurons were easily identified in the light microscope by their intense TH-antibody staining of cell bodies and neurites (Fig 3). In the allografted striatum, in the absence of a secondary spleen cell challenge, there was robust survival of TH+ cells, that was not different between weeks 10 and 21, post-grafting ($t^{1,6}$= −0.26, p= 0.81; G10: 10,348.75 ± 843.28; G21: 11,433.98 ± 4165.98; Fig 4A). Indeed, it is well established the greatest (80–95%) death of grafted TH+ neurons occurs within the first 4 days post-grafting (Duan et al., 1995;Sortwell et al., 2001). In contrast, while abundant survival of TH+ neurons was noted in the rats challenged with a spleen cell injection, there was a 64.8% decrease in the total number of TH+ neurons in this group (G21 + spleen: 3,830 ± 3486.06) compared to non-immune challenged rats. However, due to the high variability intrinsic to allogeneic models and the low number of spleen challenged rats prepared for immunohistochemistry, this difference was not statistically significant ($t^{1,6}$= 1.909, p= 0.09; Fig 4A).

The cell bodies of grafted TH+ neurons were large with plentiful cytoplasm (Fig 5A). The nucleus was round and, at the ultrastructural level, the nuclear envelope showed clear indentations. The dendrites were smooth and unlabeled neurons were found in their vicinity (Fig 5A). Fibers (Fig 5B) and punctae in the grafted striatum were considered to be outgrowths from surviving grafted cells as the lesion protocol used in this experiment produces a nigral cell loss of greater than 90% (Steece-Collier K, unpublished observation, 99.64% loss ± 0.13, n=32,). The extent of TH+ fiber re-innervation extending from the grafts was less dense than that of the intact hemisphere and diminished with increasing distance from the graft.

Host immune response—To confirm the immune status of grafted rats, we quantified the number of MHC class II+ cells in the striatum. There was a significant difference in MHC class II expression between all allografted groups ($F^{3,12}$= 4.39; Fig 4B). In non-spleen cell challenged rats, there was a non-significant change in the number (presumably due to high inter-animal variability intrinsic to allogeneic models) MHC class II+ cells from week 10 to week 21 post-grafting (G10: 351,937.98 ± 94,839; G21: 88,731.70 ± 43,601.10). In spleen cell challenged rats, the elevated level of MHC class II+ cells seen at 10 weeks post-grafting was maintained, with G21 + spleen rats showing a significantly elevated immune response compared with allografted rats sacrificed at week 21 (G21 + spleen: 754,916.24 ± 203,022.02). To examine the relationship of the host immune response to TH+ neuron loss between grafted groups, a correlation analysis of the number of TH+ neurons to the number of MHC class II+ cells in the grafted striatum was performed. No significant correlation (r = −0.37; Fig 4C) was found, suggesting a sub-lethal immune response in this particular allografted rat model.

Additional qualitative assessment at the EM level confirmed the presence of groups of microglial cells in the grafted but not the intact hemisphere in rats receiving a secondary immune challenge (G21 + spleen; Fig 5C). Further, secondary lysosomes were evident in the cytoplasm of neurons or, occasionally, in the extracellular space of the grafted striatum in G21 + spleen rats. These lysosomes were sometimes filled with membranes and dense proteinaceous bodies indicating active removal of debris (Fig 5D).

Synaptic characteristics following grafting

Synaptic connections of dopamine-grafted neurons—Electron microscopy was employed to study synaptic architecture and connections in the grafted and intact hemispheres. In both hemispheres, TH+ fibers were unmyelinated and densely filled with the flocculent DAB reaction product. All TH+ terminals were filled with large, round and pleomorphic vesicles (Fig 6A–B), while dense core vesicles were rarely seen (Fig 6A). Many TH+ synapses were formed *en passant*, typical of monoaminergic endings. As expected, there were many, unlabeled, asymmetric contacts, primarily with spines, in the intact as well as grafted striata (Fig 6A).

In the intact hemisphere, the majority of TH+ endings formed typical arrangements as symmetric inputs onto the necks of dendritic spines (spine contacts: 53.65% ± 3.25, dendritic contacts: 38.00% ± 4.86; Fig 6A–B, F), however, there was a significant change in the distribution of synaptic targets in the grafted striatum with terminals contacting significantly more dendrites than spines (χ^2= 50.683, df= 6; Fig 6C–D, F). Additionally, the distribution of synaptic targets differed significantly between allografted groups (χ^2= 37.268, df= 4). Specifically, TH+ boutons in G10 rats had equal numbers of contacts onto spines and dendrites (spine contacts: 47.02% ± 4.96; dendritic contracts: 47.98% ± 5.08), but as allografts matured (G21: spines: 34.21% ± 12.11, dendrites: 40.79% ± 14.19) the proportion of TH+ contacts onto dendrites increased significantly (G10 vs. G21: χ^2= 15.970, 2 df; Fig 6F).

To determine if the host immune response further exacerbated these synaptic changes, we compared these findings to rats challenged with spleen cell injections. Indeed, a secondary immune challenge (G21 + spleen: spine contacts: 18.51% ± 11.23, dendritic contacts: 71.48% ± 12.37) was associated with an even greater (significant) proportion of TH+ synapses contacting dendrites compared to spines (G21 vs. G21+ spleen: χ^2= 18.710, 2 df; Fig 6F).

Changes in the symmetry and the active zone length of synapses are also thought to reflect changes in synaptic function and organization (Anglade et al., 1996; Leranth et al., 1998; Meredith et al., 2000). Accordingly, we quantified the symmetry of the TH+ synapses and measured their active zone lengths. Asymmetric contacts are unusual for TH terminals, which normally form symmetric specializations (Freund et al., 1984). The current study indicates that the proportion of asymmetric to symmetric synapses does not change following allografting, however, allografted groups did differ from one another (χ^2= 36.50, df= 2) with the proportion of asymmetric synapses increasing over time (G10 vs. G21: χ^2=8.63, df= 1) and following an enhanced host immune response (G21 vs. G21 + spleen: χ^2=8.95, df= 1; percent of TH+ asymmetric synapses: G10: 4% ± 4, G21: 18% ± 11%, G21 + spleen: 38% ± 6; Fig 6G).

The mean active zone length of TH+ synapses in the grafted striata was significantly increased in all allograft striata compared to the intact sides ($F^{5,140}$= 5.549, p< 0.05; G10: 0.29μm ± 0.024, G21: 0.23μm ± 0.015, G21 + spleen: 0.25μm ± 0.022). However, immune activation did not appear to play a role in these changes as the mean active zone length of TH+ synapses in the grafted striata did not differ across groups ($F^{2,88}$= 4.821, p= 0.03; G10: 0.18μm ± 0.014, G21: 0.19μm ± 0.006, G21 + spleen: 0.21μm ± 0.01).

Synaptic input onto grafted cells—Synaptic inputs onto TH+ cell bodies and proximal dendrites were unlabeled, indicating that the inputs were not dopaminergic (Fig 7A–C). These synapses were primarily symmetric at early post-graft time points (percent of asymmetric contacts onto TH+ neurons; G10: 19.39% ± 13.57) and predominantly asymmetric with graft maturation (percent asymmetric contacts onto TH+ neurons: G21: 61.28% ± 7.95, G21 + spleen: 67.95 ± 16.06; Fig 7D).

Non-Dopaminergic Synaptic Changes Following Grafting—Quantitative analysis of asymmetric non-TH+ terminals showed a marked and significant change in the post-synaptic target of these synapses, i.e. from spine to dendritic shaft in the grafted hemisphere (χ^2= 26.80, df= 3). Specifically, in the intact striatum, over 80% of asymmetric synapses contacted spines with the remaining synapses contacting dendrites (spine contacts: 80.57% ± 2.15, dendritic contacts: 19.43% ± 2.15). In contrast, asymmetric synapses in the grafted striatum showed a significant decrease in axo-spinous contacts and a corresponding increase in axo-dendritic synapses (G10: spine contacts: 59.56% ± 10.08, dendritic contacts: 40.44% ± 10.08; G21: spine contacts: 74.60% ± 5.42, dendritic contacts: 25.40% ± 5.42; G21 + spleen: spine contacts: 50.09% ± 4.86, dendritic contacts: 49.91% ± 4.86 Figure 8A). The distribution of non TH+ targets also differed significantly amongst allografted groups (χ^2=13.40, df= 2). Interestingly, this change in relative distribution of spine and shaft synapses appeared to be related to immune activation, as rats with increased MHC class II expression (G10 and G21 + spleen rats) had a significantly greater percentage of contacts onto dendrites than spines compared with rats with a lesser immune activation (G21 rats; G10 vs. G21: χ^2= 4.47, df= 1, G21+ spleen vs. G21: χ^2=12.29, df= 1; Fig 8C).

Interestingly, the proportion of perforated asymmetric synapses increased in the grafted striata compared to the intact hemisphere (percent of perforated contacts: intact hemisphere (average): 11.77% ± 1.48, G10: 13.82% ± 4.62, G21: 13.60% ± 3.90, G21 + spleen: 20.65% ± 2.49). Perforated synapses, generally associated with increased neural activity, also differed significantly between grafted groups (χ^2= 56.20, df= 2) with the proportion of perforated synapses increasing with the increased immune response (G10 vs. G21 + spleen: χ^2= 46.87, df= 1) but not with graft maturation (G10 vs. G21: χ^2=35.02, df= 1; Fig 8D).

Synaptic alterations correlate with novel dyskinesias—Correlation analyses were performed to determine if any of the synaptic changes observed in rats of varying immune status were associated with GIDs occurrence or severity (Table 1). Overall, there were significant correlations between certain changes in synaptic features and particular aspects of GIDs-like behaviors. First, tapping dyskinesia was negatively correlated with the proportion of TH+ synapses onto dendritic spines (r= −0.65; Fig 9); that is, the fewer the axo-spinous contacts, the greater the degree of tapping dyskinesias. Second, total GIDs severity showed a significant positive correlation with the proportion of asymmetric synapses onto TH+ grafted cells (r= 0.73; Fig 10). Third, an increase in the percent of non-TH+, asymmetric, perforated synapses correlated significantly with an increase in the occurrence of total GIDs severity (r= 0.57; Fig 11).

The correlation between the percent of atypical asymmetric contacts made by TH+ contacts onto host neurons and total GIDs severity showed a positive trend, but a statistically significant correlation was not found. Likewise, the change in non-TH+ asymmetric synaptic targets (i.e.: spine versus dendrite) did not correlate significantly with any of the observed behaviors. Taken together, the significant correlations found in this study support the hypothesis that specific aberrant synaptic features found following activation of the host immune response in allografted rats modulate the occurrence of GIDs.

Discussion

This study is the first to demonstrate that aberrant synaptic features in the parkinsonian striatum of rats following dopaminergic cell grafting are associated with the expression of graft-mediated motor dysfunction. While abnormalities in the synaptic connections of grafted dopaminergic neurons have previously been documented (e.g. Freund et al., 1985; Mahalik et al., 1985, Leranth et al., 1998), the biological contributors to this reorganization and behavioral consequences remain obscure. We show that allografted dopaminergic neurons, in the presence

of an elevated host immune response, show significant increases in aberrant synaptic features (summarized in table 1 and figure 13), many of which correlate statistically with the severity of graft-induced behaviors. These data suggest that synaptic reorganization contributes to the evolution of aberrant motor behaviors and is associated with the host immune response.

Dichotomy of Dopaminergic Grafts

In patients, dopaminergic grafts decrease LIDs while inducing GIDs (Freed et al., 2001; Hagell et al., 2002; Olanow et al., 2003). Recent studies have demonstrated the ability to recapitulate some aspects of GIDs in a parkinsonian rat model (Steece-Collier et al., 2003; Maries et al., 2006; Lane et al., 2006; Carlsson et al., 2006). While differences exist between GIDs in clinical trials and the rat model, in both these behaviors emerge with graft maturation, tend to be focal and stereotypic, and increase in expression despite decreased LIDs (Hagell et al., 2002; Olanow et al., 2003; Maries et al., 2006; Lane et al., 2006). In the present study, the number of surviving, grafted TH+ cells correlated with a reduction in LIDs, a finding similar to that of Lane and colleagues (2006), but not with the severity of GIDs. Indeed, there was a trend towards a further reduction in LIDs after a second spleen cell injection, which could be related to trophic influences of some immune factors. Moreover, LIDs were not correlated with any observed synaptic feature, whereas GIDs were significantly correlated with atypical synaptic connections between graft and host tissues (Fig. 12). The differential relationship of these two behavioral abnormalities to select post-graft parameters supports the hypothesis that LIDs and GIDs represent distinct neurological entities (Hagell and Cenci, 2005), with distinct underlying mechanisms.

Synaptic Reorganization and Behavioral Consequences

Dopaminergic terminals in the normal striatum predominantly synapse onto the neck, and glutamatergic endings onto the head, of dendritic spines (Freund et al., 1984; Groves et al., 1980). Dopamine depletion leads to a significant loss of dendritic spines (McNeill et al., 1988; Ingham et al., 1998; Zaja-Milatovic et al., 2005; Stephens et al., 2005; Day et al., 2006); thus, it is not surprising that grafted dopaminergic neurons form new synapses with dendrites more often than spines (Freund et al., 1985, Mahalik et al., 1985, Bolam et al., 1988, Clarke et al., 1989, Stromberg et al., 1990, Triarhou et al., 1990). In the current study, we find that this change in target is enhanced with immune activation and statistically correlates with graft-induced motor abnormalities.

Symmetric specializations are classically associated with inhibitory, and asymmetric with excitatory, neurotransmission (Peters and Palay, 1996). Striatal dopaminergic terminals predominantly make symmetric, but rarely asymmetric synapses (Freund et al., 1984). In the current study, the proportion of TH+ synapses making asymmetric specialization was significantly increased in the allografted parkinsonian striatum. The idea that dopaminergic neurons make two morphologically distinct types of synapses has been extensively debated (Hattori 1993; Groves et al., 1994; Sulzer et al., 1998). Several lines of evidence have demonstrated that central monoaminergic neurons including nigral dopaminergic neurons in rat and monkey brain are capable of glutamatergic co-transmission (reviewed in Sulzer et al., 1998). Indeed, stimulation of single, dopaminergic neurons in microculture can evoke calcium-dependent excitatory postsynaptic potentials (Sulzer et al., 1998). An increase in the number of asymmetric synapses formed by grafted dopaminergic neurons, also seen in the grafted parkinsonian monkey striatum (Leranth et al., 1998), could further alter striatal activity within grafted regions.

Excitatory asymmetric synapses in striatum are critical for learning and adaptive or goal-directed motor behaviors, but can also underlie pathological learning associated with dyskinesias and/or motor tics (Picconi et al., 2003; Mink, 2003). In the current study, unlabeled

asymmetric synapses contacted the cell bodies and proximal dendrites of the grafted cells. Such connections were correlated statistically with an increased incidence of GIDs-like behaviors. These synapses may be new corticostriatal endings (Arbuthnott et al., 1985; Fisher et al., 1991), that would be expected to stimulate grafted cells, potentially accounting for the irregular spontaneous discharge and fast firing rate of grafted dopaminergic neurons (Trulson and Hosseini, 1987; Fisher et al., 1991).

The current study also demonstrated an increase in perforated, asymmetric synapses, which correlated statistically with GIDs-like behaviors. Perforated synapses are associated with elevated excitatory activity and long-term potentiation (LTP; Marrone and Petit, 2002), a form of synaptic plasticity dysregulated in dyskinesia. In PD patients (Morgante et al., 2006; Picconi et al., 2008) and parkinsonian rats (Picconi et al., 2005), LTP plasticity is deficient. Levodopa administration results in the recovery of striatal LTP, however, restoration of synaptic depotentiation, a process that reverses LTP and is required to “erase redundant information”, is deficient in dyskinetic subjects (e.g.: Picconi et al., 2005). It is possible that increased perforated synapses in the allografted striatum represent aberrant LTP-related plasticity that promote dyskinesias.

Potential mechanisms

The continued survival of allografted TH+ cells and attenuation of LIDs in the presence of an activated host immune response suggests that immune-mediated behavioral and synaptic modifications occurred through sub-lethal effects as opposed to an outright loss of grafted cells. However, some degree of sub-lethal toxicity could have resulted in the development of graft-derived dopaminergic “hot-spots”. Our lab has previously reported that focal, but not widespread, dopaminergic grafts induced expression of GIDs-type behaviors in parkinsonian rats (Maries et al., 2006). In the present study, hotspots of dopaminergic activity could have resulted from the large complement of host, asymmetric synapses innervating the perisomatic regions of the TH+ grafted cells. Further, excessive, localized excitatory signaling could have been enhanced through the increased number of asymmetric synapses made by grafted TH+ cells onto host neurons. Additionally, recent studies showed that inflammation elicits aberrant cellular responses thorough inappropriate signaling. Specifically, dimerization of cytokine receptors leads to receptor-receptor interactions with dopaminergic neurons and subsequent aberrant signaling (e.g. Fuxe et al., 2008). However, our findings that GIDs-like behaviors occurred only in dopamine-grafted rats, and not in cell-free, sham-grafted rats, despite the presence of equal numbers of MHC class II+ cells in sham and G21 rats, suggests that the impact of host immune factors are more likely to be related to graft-host synaptic organization than to a direct action on host signaling pathways.

There is strong evidence to support a role for pro-inflammatory factors in synaptic plasticity of neural circuits under normal and pathological conditions (see Leonardo et al., 2005 for review). Inflammatory cytokines have been linked to increased induction of activation-associated genes, including components of the AP-1 family of transcription factors (Kyriakis et al., 1999), such as FosB/ΔFosB, a transcription factor upregulated in animal models of dyskinesias (Cenci, 2002; Maries et al., 2006). Data from other models of inflammation have shown elevated expression of genes involved in synaptogenesis (Yukhananov and Kissin, 2008), and microglial activation associated with synaptic stripping (Rasmussen et al., 2007). Inflammation may therefore interfere with the formation of appropriate synaptic contacts by grafted or host neurons. In our study, a hallmark feature of strengthened synapses, synaptic perforation, was significantly increased in the grafted rats that developed GIDs. This finding may be explained by the actions of the inflammatory cytokine, tumor necrosis factor alpha (TNFα), which triggers long-lasting increases in synaptic strength and influences AMPA receptor trafficking (Beattie et al., 2002; Bains et al., 2007).

The structural findings of the current study provide insight into a potential mechanistic link that supports continued investigation into how, and which, immune factors mediate graft-host interactions. In addition, it will be important to examine whether aberrant synaptic profiles, suggestive in this study of excessive excitatory activity within the grafted striatum, are linked to altered neuronal excitability that could give rise to aberrant focal output. It is well known that localized stimulation of striatum results in focal output of stereotyped behavior, which is dependent upon which area of striatum is stimulated (Mink 2003; Kelley et al. 1994).

Considerations for clinical grafting

The current study shows that the immune system is associated with the formation of aberrant synaptic features between grafted dopaminergic neurons and host MSNs in a parkinsonian rat model. These findings, in addition to abundant evidence supporting a role for pro-inflammatory factors in synaptic plasticity (see Leonardo et al., 2005 for review), and the emergence of GIDs in grafted PD patients following the withdrawal from immune suppression (Olanow et al., 2003; Piccini et al., 2005), suggest that the role of the host immune system in cell replacement therapies warrants further investigation. Additional factors, such as the loss of important input targets for newly grafted cells (dendritic spines) could lead to aberrant host-graft connectivity, suboptimal behavioral efficacy, and the generation of GIDs.

Acknowledgments

The authors would like to thank Dr. Wei-Ming Duan of Louisiana State University, for his valuable suggestions regarding spleen cell injections. We would also like to thank the statisticians at Rush University, in particular Dr. Sue Leurgans, for their guidance with our data analyses. Further, we would like to acknowledge the outstanding technical assistance of Nathan Levine, Jennifer Stancati and Brian Daley, and the support of the Electron Microscopy Center at Rosalind Franklin University. This work was supported in part by: the Michael J. Fox Foundation (KSC); the Department of Defense Neurotoxin Exposure Treatment Research Program (KSC); and the National Institutes Neurological Disorders and Stroke (KSC).

References

Anglade P, Mouatt-Prigent A, Agid Y, Hirsch E. Synaptic plasticity in the caudate nucleus of patients with Parkinson's disease. Neurodegeneration 1996;5:121–8. [PubMed: 8819132]

Arbuthnott G, Dunnett S, MacLeod N. Electrophysiological properties of single units in dopamine-rich mesencephalic transplants in rat brain. Neurosci Lett 1985;57:205–10. [PubMed: 2993967]

Bains JS, Oliet SH. Glia: they make your memories stick! Trends Neurosci 2007;30:417–24. [PubMed: 17631972]

Beattie EC, Stellwagen D, Morishita W, Bresnahan JC, Ha BK, Von Zastrow M, Beattie MS, Malenka RC. Control of synaptic strength by glial TNF alpha. Science 2002;295:2282–5. [PubMed: 11910117]

Bolam JP. Synapses of identified neurons in the neostriatum. Ciba Found Symp 1984;107:30–47. [PubMed: 6149899]

Bolam JP, Izzo PN. The postsynaptic targets of substance P-immunoreactive terminals in the rat neostriatum with particular reference to identified spiny striatonigral neurons. Exp Brain Res 1988;70:361–77. [PubMed: 2454839]

Carlsson T, Winkler C, Lundblad M, Cenci MA, Bjorklund A, Kirik D. Graft placement and uneven pattern of reinervation in the striatum is important for development of graft-induced dyskinesia. Neurobiol Dis 2006;21:657–68. [PubMed: 16256359]

Cenci MA. Transcription factors involved in the pathogenesis of L-DOPA-induced dyskinesia in a rat model of Parkinson's disease. Amino Acids 2002;23:105–9. [PubMed: 12373525]

Clarke DJ, Brundin P, Strecker RE, Nilsson OG, Bjorklund A, Lindvall O. Human fetal dopamine neurons grafted in a rat model of Parkinson's disease: ultrastructural evidence for synapse formation using tyrosine hydroxylase immunocytochemistry. Exp Brain Res 1988;73:115–26. [PubMed: 3145209]

Day M, Wang Z, Ding J, AN X Ingham CA, Shering A, Wokosin D, Ilijic E, Sun Z, Sampson AR, Mugnaini E, Deutch AY, Sesack SR, Arbuthnott GW, Surmeier DJ. Selective elimination of

glutamatergic synapses on striatopallidal neurons in Parkinson's disease models. Nat Neurosci 2006;9:251–9. [PubMed: 16415865]

DeFelipe J, Conti F, Van Eyck SL, Manzoni T. Demonstration of glutamate-positive axon terminals forming asymmetric synapses in cat neocortex. Brain Res 1988;455:162–5. [PubMed: 3416182]

Di Loreto S, Florio T, Capozzo A, Napolitano A, Adorno D, Scarnati E. Transplantation of mesencephalic cell suspension in dopamine-denervated striatum of the rat. Exp Neurol 1996;138:318–26.

Duan WM, Widner H, Frodl EM, Brundin P. Immune reactions following systemic immunization prior or subsequent to intrastriatal transplantation of allogeneic mesencephalic tissue in adult rats. Neuroscience 1995a;64:629–41. [PubMed: 7715776]

Duan WM, Widner H, Brundin P. Temporal pattern of host responses against intrastriatal grafts of syngeneic, allogeneic, or xenogeneic embryonic neuronal tissue in rats. Exp Brain Res 1995b; 104:227–42. [PubMed: 7672016]

Duan WM, Brundin P, Widner H. Addition of allogeneic spleen cells causes rejection of intrastriatal embryonic mesencephalic allografts in the rat. Neuroscience 1997;77:599–609. [PubMed: 9472415]

Eljaschewitsch E, Witting A, Mawrin C, Lee T, Schmidt PM, Wolf S, Hoertnagl H, Raine CS, Schneider-Stock R, Nitsch R, Ullrich O. The endocannabinoid anandamide protects neurons during CNS inflammation by induction of MKP-1 in microglial cells. Neuron 2006;49:67–79. [PubMed: 16387640]

Fahn S. The spectrum of levodopa-induced dyskinesias. Ann Neurol 2000;47:S2–9. [PubMed: 10762127]

Fisher LJ, Young SJ, Tepper JM, Groves PM, Gage FH. Electrophysiological characteristics of cells within mesencephalon suspension grafts. Neuroscience 1991;40:109–22. [PubMed: 2052146]

Freed CR, Greene PE, Breeze RE, Tsai WY, DuMouchel W, Kao R, Dillon S, Winfield H, Culver S, Trojanowski JQ, Eidelberg D, Fahn S. Transplantation of embryonic dopamine neurons for severe Parkinson's disease. N Engl J Med 2001;344:710–9. [PubMed: 11236774]

Freund TF, Powell JF, Smith AD. Tyrosine hydroxylase-immunoreactive boutons in synaptic countact with identified striatonigral neurons, with particular reference to dendritic spines. Neuroscience 1984;13:1189–215. [PubMed: 6152036]

Freund TF, Bolam JP, Bjorklund A, Stenevi U, Dunnett SB, Powell JF, Smith AD. Efferent synaptic connections of grafted dopaminergic neurons reinnervating the host neostriatum: a tyrosine hydroxylase immunocytochemical study. J Neurosci 1985;5:603–16. [PubMed: 2857778]

Fuxe KG, Tarkanov AO, Goncharova LB, Agnati LF. A new road to neuroinflammation in Parkinson's disease? Brain Res Rev. 2008 [Epub ahead of print].

Gerfen CR. Synaptic organization of the striatum. J Electron Microsc Tech 1988;10:265–81. [PubMed: 3069970]

Glezer I, Simard AR, Rivest S. Neuroprotective role of the innate immune system by microglia. Neuroscience 2007;147:867–83. [PubMed: 17459594]

Groves PM. Synaptic endings and their postsynaptic targets in neostriatum: synaptic specializations revealed from analysis of serial sections. Proc Natl Acad Sci USA 1980;77:6926–9. [PubMed: 6935693]

Groves PM, Linder JC, Young SJ. 5-hydroxydopamine-labeled dopaminergic axons: three-dimensional reconstructions of axons, synapses and postsynaptic targets in rat neostriatum. Neuroscience 1994;58:593–604. [PubMed: 8170539]

Gundersen HJ. Stereology of arbitrary particles. A review of unbiased number and size estimators and the presentation of some new ones, in memory of William R. Thompson. J Microsc 1986;143:3–45. [PubMed: 3761363]

Hagell P, Piccini P, Bjorklund A, Brundin P, Rehnscrona S, Widner H, Crabb L, Pavese N, Oertel WH, Quinn N, Brooks DJ, Lindvall O. Dyskinesias following neural transplantion in Parkinson's disease. Nat Neurosci 2002;5:627–8. [PubMed: 12042822]

Hagell P, Cenci MA. Dyskinesias and dopamine cell replacement in Parkinson's disease: a clinical perspective. Brain Res Bull 2005;68:4–15. [PubMed: 16324999]

Hattori T. Conceptual history of the nigrostriatal dopamine system. Neurosci Res 1993;16:239–62. [PubMed: 8394552]

Ingham CA, Hood SH, van Maldegem B, Weenink A, Arbuthnott GW. Morphological changes in the rat neostriatum after unilateral 6-hydroxydopamine injections into the nigrostriatal pathway. Exp Brain Res 1993;93:17–27. [PubMed: 7682182]

Ingham CA, Hood SH, Taggart P, Arbuthnott GW. Plasticity of synapses in the rat neostriatum after neostriatum after unilateral lesion of the nigrostriatal dopaminergic pathway. J Neurosci 1998;18:4732–43. [PubMed: 9614247]

Kelley AE, Lang CG, Gauthier AM. Induction of oral stereotypy following amphetamine microinjection into a discrete subregion of the striatum. Psychopharmacology (Berl) 1988;95:556–9. [PubMed: 3145527]

Kyriakis JM, Avruch J. Sounding the alarm: protein kinase cascades activated by stress and inflammation. J Biol Chem 1999;271:24313–6. [PubMed: 8798679]

Lane EL, Winkler C, Brundin P, Cenci MA. The impact of graft size on the development of dyskinesia following intrastriatal grafting of embryonic dopamine neurons in the rat. Neurobiol Dis 2006;22:334–45. [PubMed: 16406222]

Leonardo A. Degenerate coding in neural systems. J Comp Physiol A Neuroethol Sens Neural Behav Physiol 2005;191:995–1010. [PubMed: 16252121]

Leranth C, Sladek JR Jr, Roth RH, Redmond DE Jr. Efferent synaptic connections of dopaminergic neurons grafted into the caudate nucleus of experimentally induced parkinsonian monkeys are different from those of control animals. Exp Brain Res 1998;123:323–33. [PubMed: 9860271]

Lindefors N, Ungerstedt U. Bilateral regulation of glutamate tissue and extracellular levels in caudate-putamen by midbrain dopamine neurons. Neurosci Lett 1990;115:248–52. [PubMed: 1978265]

Ma Y, Feigin A, Dhawan V, Fukuda M, Shi Q, Greene P, Breeze R, Fahn S, Freed C, Eidelberg D. Dyskinesia after fetal cell transplantation for parkinsonism: a PET study. Ann Neurol 2002;52:628–34. [PubMed: 12402261]

Mahalik TJ, Finger TE, Stromberg I, Olson L. Substantia nigra transplants into denervated striatum of the rat: ultrastructure of graft and host interconnections. J Comp Neurol 1985;240:60–70. [PubMed: 2865279]

Maries E, Kordower JH, Chu Y, Collier TJ, Sortwell CE, Olaru E, Shannon K, Steece-Collier K. Focal not widespread grafts induce novel dyskinetic behavior in parkinsonian rats. Neurobiol Dis 2006;21:165–80. [PubMed: 16095907]

Marrone DF, Petit TL. The role of synaptic morphology in neural plasticity: structural interactions underlying synaptic power. Brain Res Brain Res Rev 2002;38:291–308. [PubMed: 11890978]

McNeill TH, Brown SA, Rafols JA, Shoulson I. Atrophy of medium spiny I striatal dendrites in advanced Parkinson's disease. Brain Res 1988;455:148–52. Ingham et al., 1989. [PubMed: 3416180]

Meredith GE, De Souza IE, Hyde TM, Tipper G, Wong ML, Egan MF. Persistent alterations in dendrites, spines, and dynorphinergic synapses in the nucleus accumbens shell of rats with neuroleptic-induced dyskinesias. J Neurosci 2000;20:7798–806. [PubMed: 11027244]

Meshul CK, Emre N, Nakamura CM, Allen C, Donohue MK, Buckman JF. Time-dependent changes in striatal glutamate synapses following a 6-hydroxydopamine lesion. Neuroscience 1999;88:1–16. [PubMed: 10051185]

Mink JW. The basal ganglia and involuntary movements: impaired inhibition of competing motor patterns. Arch Neurol 2003;60:1365–8. [PubMed: 14568805]

Morgante F, Espay AJ, Gunraj C, Lang AE, Chen R. Motor cortex plasticity in Parkinson's disease and levodopa-induced dyskinesias. Brain 2006;129:1059–69. [PubMed: 16476674]

Olanow CW, Goetz CG, Kordower JH, Stoessl AJ, Sossi V, Brin MF, Shannon KM, Nauert GM, Perl DP, Godbold J, Freeman TB. A double-blind controlled trial of bilateral fetal nigral transplantation in Parkinson's disease. Ann Neurol 2003;54:403–14. [PubMed: 12953276]

Paxinos, G. The Rat Nervous System. New York, NY: Elsevier Academic Press; 2004.

Peters A, Palay SL. The morphology of synapses. J Neurocytol 1991;25:687–700. [PubMed: 9023718]

Piccini P, Pavese N, Hagell P, Reimer J, Bjorklund A, Oertel WH, Quinn NP, Brooks DJ, Lindvall O. Factors affecting the clinical outcome after neural transplantation in Parkinson's disease. Brain 2005;128:2977–86. [PubMed: 16246865]

Picconi B, Centonze D, Hakansson K, Bernardi G, Greengard P, Fisone G, Cenci MA, Clabresi P. Loss of bidirectional striatal synaptic plasticity in L-DOPA-induced dyskinesia. Nat Neurosci 2003;6:501–6. [PubMed: 12665799]

Picconi B, Pisani A, Barone I, Bonsi P, Centonze D, Bernardi G, Calabresi P. Pathological synaptic plasticity in the striatum: implications for Parkinson's disease. Neurotoxicology 2005;26:779–83. [PubMed: 15927256]

Picconi B, Paille V, Ghiglieri V, Bagetta V, Barone I, Lindgren H, Bernardi G, Cenci MA, Calabresi P. L-DOPA dosage is critically involved in dyskinesia via loss of synaptic depotentiation. Neurobiol Dis 2008;29:327–35. [PubMed: 17997101]

Pickel VM, Beckley SC, Sumal KK, Joh TH, Reis DJ, Miller RJ. Light and electron microscopic localization of enkephalin and tyrosine hydroxylase in neostriatum of fetal and adult rat brain. Acta Histochem Suppl 1981;24:97–105. [PubMed: 6112776]

Rasmussen S, Wang Y, Kivisakk P, Bronson RT, Meyer M, Imitola J, Khoury SJ. Persistent activation of microglia is associated with neuronal dysfunction of callosal projecting pathways and multiple sclerosis-like lesions in relapsing-remitting experimental autoimmune encephalomyelitis. Brain 2007;130:2816–29. [PubMed: 17890734]

Sortwell CE, Camargo MD, Pitzer MR, Gyawali S, Collier TJ. Diminished survival of mesencephalic dopamine neurons grafted into aged hosts occurs during the immediate postgrafting interval. Exp Neurol 2001;169:23–9. [PubMed: 11312554]

Steece-Collier K, Collier TJ, Danielson PD, Kurlan R, Yurek DM, Sladek JR Jr. Embryonic mesencephalic grafts increase levodopa-induced forelimb hyperkinesia in parkinsonian rats. Mov Disord 2003;18:1442–54. [PubMed: 14673880]

Stephens B, Mueller AJ, Shering AF, Hood SH, Taggart P, Arbuthnott GW, Bell JE, Kilford L, Kingsbury AE, Daniel SE, Ingham CA. Evidence of a breakdown of corticostratal connections in Parkinson's disease. Neuroscience 2005;132:741–54. [PubMed: 15837135]

Stromberg I, Kehr J, Andbjer B, Fuxe K. Fetal ventral mesencephalic grafts functionally reduce the dopamine D2 receptor supersensitivity in partially dopamine reinnervated host striatum. Exp Neurol 2000;1164:154–165. [PubMed: 10877926]

Sulzer D, Joyce MP, Lin L, Geldwert D, Haber SN, Hattori T, Rayport S. Dopamine neurons make glutamatergic synapses in vitro. J Neurosci 1998;18:4588–602. [PubMed: 9614234]

Tonelli LH, Postolache TT, Sternberg EM. Inflammatory genes and neural activity: involvement of immune genes in synaptic function and behavior. Front Biosci 2005;10:675–80. [PubMed: 15569608]

Triarhou LC, Brundin P, Doucet G, Norton J, Bjorklund A, Ghetti B. Intrastriatal implants of mesencephalic cell suspensions in weaver mutant mice: ultrastructural relationships of dopaminergic dendrites and axons issued from the graft. Exp Brain Res 1990;79:3–17. [PubMed: 1968850]

Trulson ME, Hosseini A. Dopamine neuron transplants: electrophysiological unit activity of intrastriatal nigral grafts in freely moving cats. Life Sci 1987;40:2097–102. [PubMed: 3586853]

Yamamoto BK, Davy S. Dopaminergic modulation of glutamate release in striatum as measured by microdialysis. J Neurochem 1992;58:1736–42. [PubMed: 1348523]

Yukhananov R, Kissin I. Persistent changes in spinal cord gene expression after recovery from inflammatory hyperalgesia: a preliminary study on pain memory. BMC Neurosci 2008;9:32. [PubMed: 18366630]

Zaja-Milatovic S, Milatovic D, Schantz AM, Zhang J, Montine KS, Samii A, Deutch AY, Montine TJ. Dendritic degeneration in neostriatal medium spiny neurons in Parkinson's disease. Neurology 2005;64:545–7. [PubMed: 15699393]

GROUP	Sham	G10	G21	G21 + spleen
TREATMENT	Ungrafted	Allograft, sac'd @ 10 weeks	Allograft, sac'd @ 21 weeks	Allograft + spleen, sac'd @ 21 weeks
N	16	4 (for EM) 4 (for IHC)	4 (for EM) 4 (for IHC)	4 (for EM) 5 (for IHC)
IMMUNE RESPONSE	None	Moderate	Moderate	High

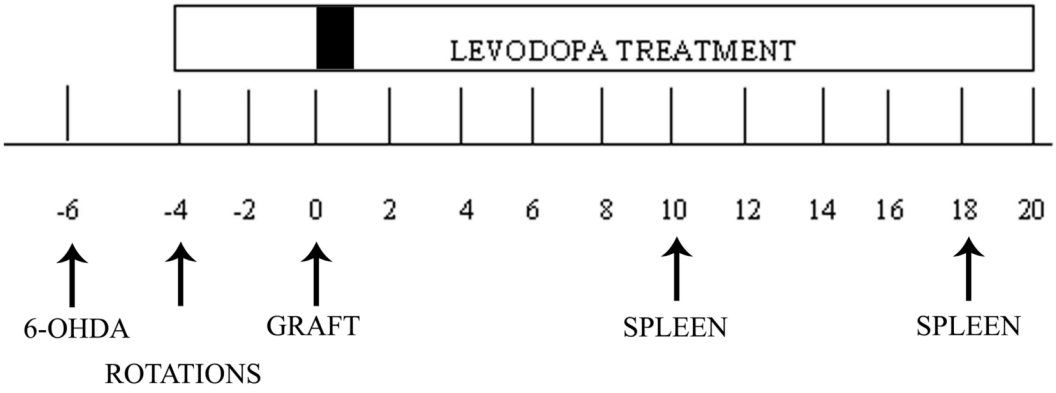

Figure 1. Experimental Groups and Timeline

Rats were placed into 3 treatment groups; sham group (ungrafted), allografted group sacrificed at 21 weeks (G21), and allografted group receiving peripheral spleen cells injections (G21 + spleen) sacrificed at 21 weeks. An additional cohort of rats (N=8) was sacrificed at a 10-week post-graft time point to serve for mid-point (pre-spleen) assessment of graft and immune cell integrity. All rats received unilateral nigrostriatal 6-OHDA lesions, which were confirmed 2 weeks later with amphetamine-induced rotational testing. Rats were primed with levodopa 4 weeks prior to neural grafting (one week of a priming dose of 25mg/kg levodopa, 25mg/kg benserazide, followed by 3 weeks of 12.5 mg/kg levodopa, 12.5mg/kg benserazide; once daily, 5 days a week). Rats were grafted 6 weeks following 6-OHDA. Levodopa treatment was withheld from all rats for one week post-grafting followed by weekly delivery of 12.5mg/kg levodopa, 12.5mg/kg benserazide once daily, 5 days a week for the remainder of the experiment. G21 + spleen treated rats received peripheral, subcutaneous spleen cell injections on weeks 10 and 18 post-grafting.

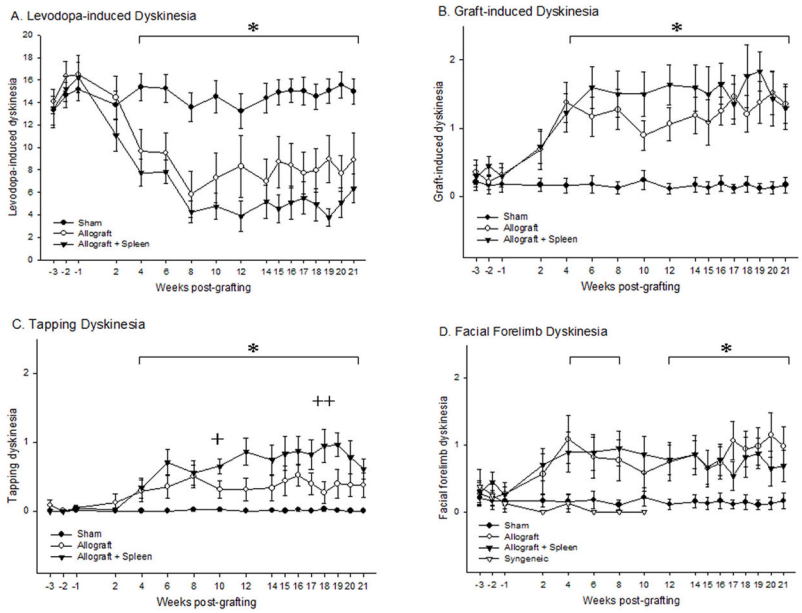

Figure 2. Levodopa and Graft-induced Dyskinetic Behavioral Profiles

(A) Levodopa-induced dyskinesias (LIDs) for all groups over 21 weeks. A significant difference was seen between both allografted groups and the sham group by week 4 post-grafting (*p<0.05). Rats receiving peripheral spleen cell injections (G21+ spleen) showed a trend toward greater improvement (p=0.053) in LIDs compared to rats receiving allografts alone (G21) following secondary immune challenge. (B) Total graft-induced dyskinesias (GIDs; tapping dyskinesias + facial forelimb dyskinesias) for all groups over 21 weeks. The emergence of novel (e.g.: not seen prior to grafting) dyskinetic behaviors was noted in all allografted rats and was significantly increased over sham treated rats by week 4 post-grafting (*p<0.05). (C) Tapping dyskinesias phenotype showed a significant increase in all allografted rats by 4 weeks post-grafting compared to sham-treated rats (*p<0.05). There was a further augmentation in this behavioral phenotype in the G21 + spleen group, compared with G21 group on weeks 10 (+p=0.03) and 18 (++p=0.01) post-grafting. (D) Facial forelimb dyskinesias phenotype showed a significant increase in all allografted rats at 4 weeks post-grafting compared to sham-treated rats (*p<0.05). Syngeneic-grafted rats observed in a previous study in our laboratory, undergoing the identical experimental protocol as used for allografted rats in this study, failed to develop post-graft motor abnormalities (D).

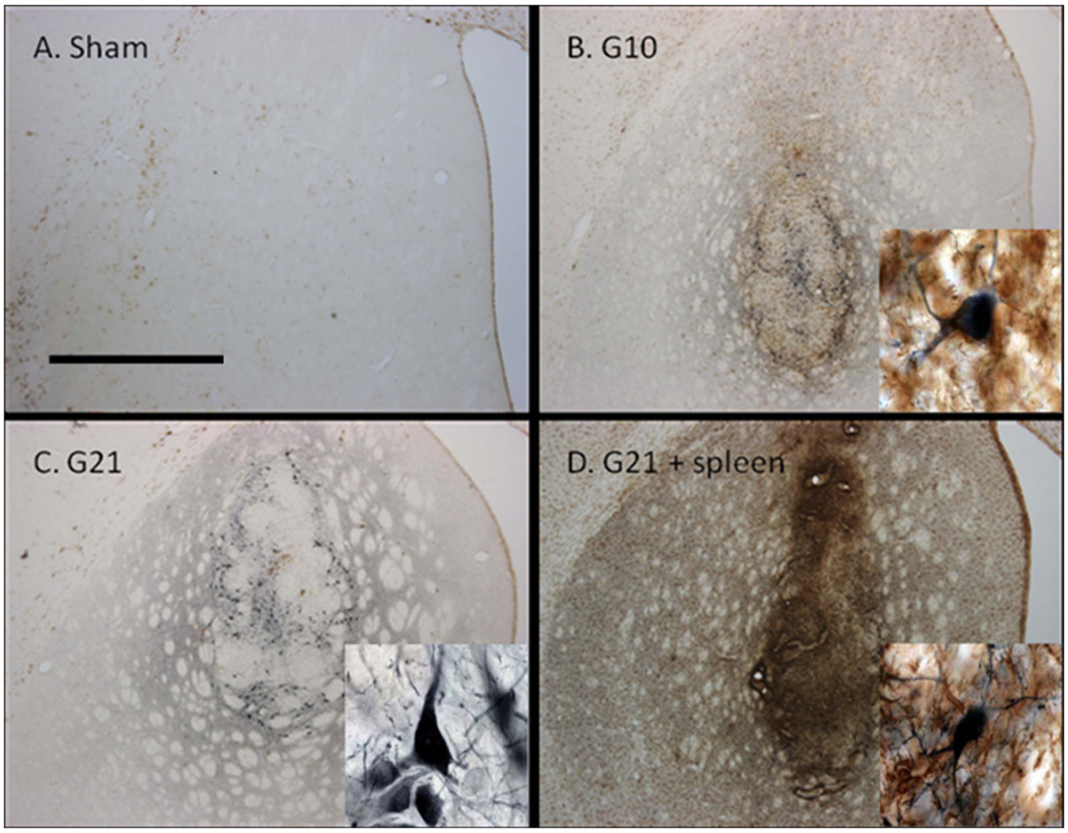

Figure 3. Tyrosine hydroxylase (TH, blue) and MHC class II molecule (MHC II, brown) immunostained, coronal brain sections in the dopamine-depleted striatum

A) Sham treated rats showed an absence of TH innervation and sparse MHC class II expression. B) Allografted rats sacrificed at 10 weeks post-grafting (G10) showed numerous TH+ cells as well as moderate MHC class II expression at the site of the graft. C) Allografted rats sacrificed on week 21 post-grafting (G21) showed abundant TH+ cells and a reduced expression MHC class II expression compared to G10. D) Allografted rats receiving peripheral spleen cell injections and sacrificed at 21 weeks (G21 + spleen) showed some remaining TH+ cells and robust MHC class II expression. Scale bar in A represents 1mm and is valid for A–D.

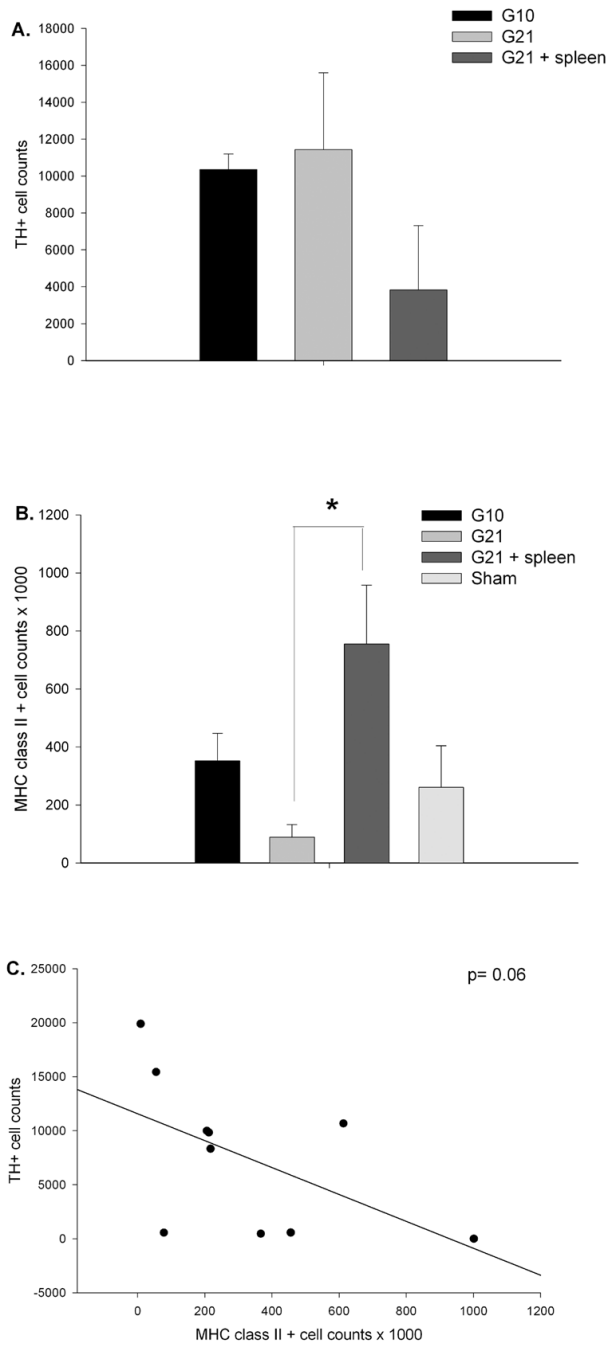

Figure 4. Tyrosine hydroxylase and MHC class II cell counts

(A) While there was approximately 50% fewer TH+ cells in the DA-depleted striatum of spleen challenged allografted rats, there was no statistical difference between the allograft groups ($p = 0.45$). (B) The number of MHC class II+ cells in the DA-depleted striatum differed significantly between groups ($p=0.03$) with G21 + spleen rats showing significantly more compared to G21 rats (*$p < 0.05$). (C) While there was a trend for higher numbers of MHC class II+ cells to be associated with lower numbers of surviving TH+ cells this correlation was not statistically significant ($r=-0.37$, $p=0.06$).

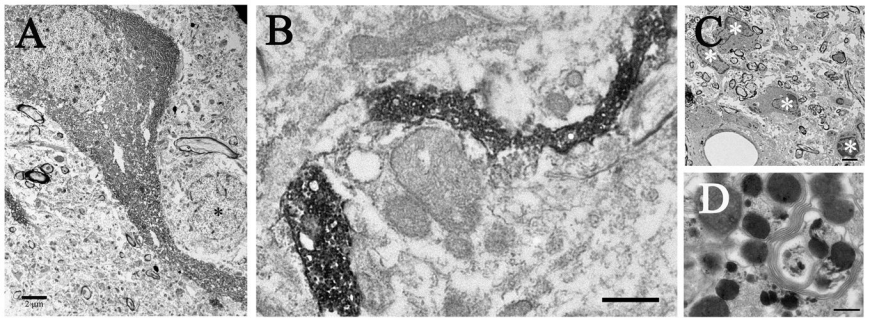

Figure 5. Electron micrographs of the dopamine-depleted striatum illustrating the presence of grafted dopaminergic neurons (A), fibers (B), and the host inflammatory response (C–D)

(A) Low power ultrastructure micrograph of a dopaminergic neuron showing close proximity to a small interneuron (*), which can be identified by the deep indentations in the nuclear envelop. Scale bar= 2μm. (B) Low power micrograph of a TH+ fiber coursing through the extracellular space. (C) Low power micrograph of microglia (*) found in the striatum of a G21 + spleen rat. (D) High power micrograph of a large secondary lysosome filled with debris, dense protein, and parallel membranes. Scale bar in C= 2μm and D= 250nm.

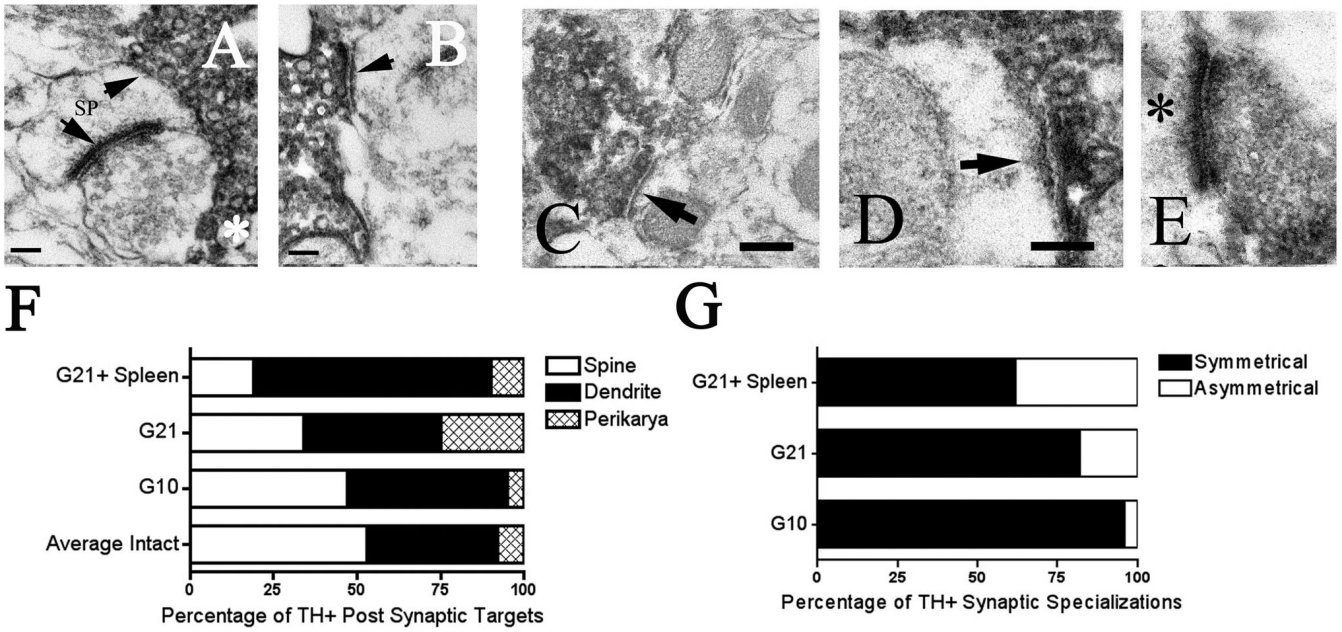

Figure 6. Electron micrographs of synaptic profiles in the intact and grafted striatum

A, B*) In the intact hemisphere* synapses formed typical arrangements with TH+ terminals forming symmetric contacts (A: upper arrow, B: arrow) onto spines (A: upper arrow, B: arrow) and non-TH+ asymmetric synapses (A: lower arrow) forming contacts onto the head of the spine. Note the dense core vesicles in the TH+ terminal (A: asterisk). Scale bar for A and B=100nm. C, D) *In the grafted hemisphere* TH+ synapses showed more atypical arrangements sometimes forming asymmetric contacts (high power micrographs D and E: arrow and asterisk) and often contacting dendrites as opposed to spines (low power micrograph C: arrow; high power micrograph D: arrow). *Figures F and G show schematic diagrams* of this change in distribution of TH+ synaptic target (F) and synaptic specialization (G) between the intact and grafted striata. (F) The distribution of synaptic targets in the grafted striata differed significantly from the intact hemisphere ($p < 0.001$), as well as from one another, ($p < 0.001$; G10 vs. G21: $p<0.001$, G10 vs. G21 + spleen: $p< 0.001$, G21 vs. G21 + spleen: $p<0.001$). (G) The distribution of synaptic symmetry also differed significantly between allografted groups ($p<0.001$; G10 vs. G21: $p= 0.003$, G10 vs. G21 + spleen: $p< 0.001$, G21 vs. G21 + spleen: $p= 0.003$) with the percent of TH+ asymmetric specializations increasing with both time post-grafting and host immune response.

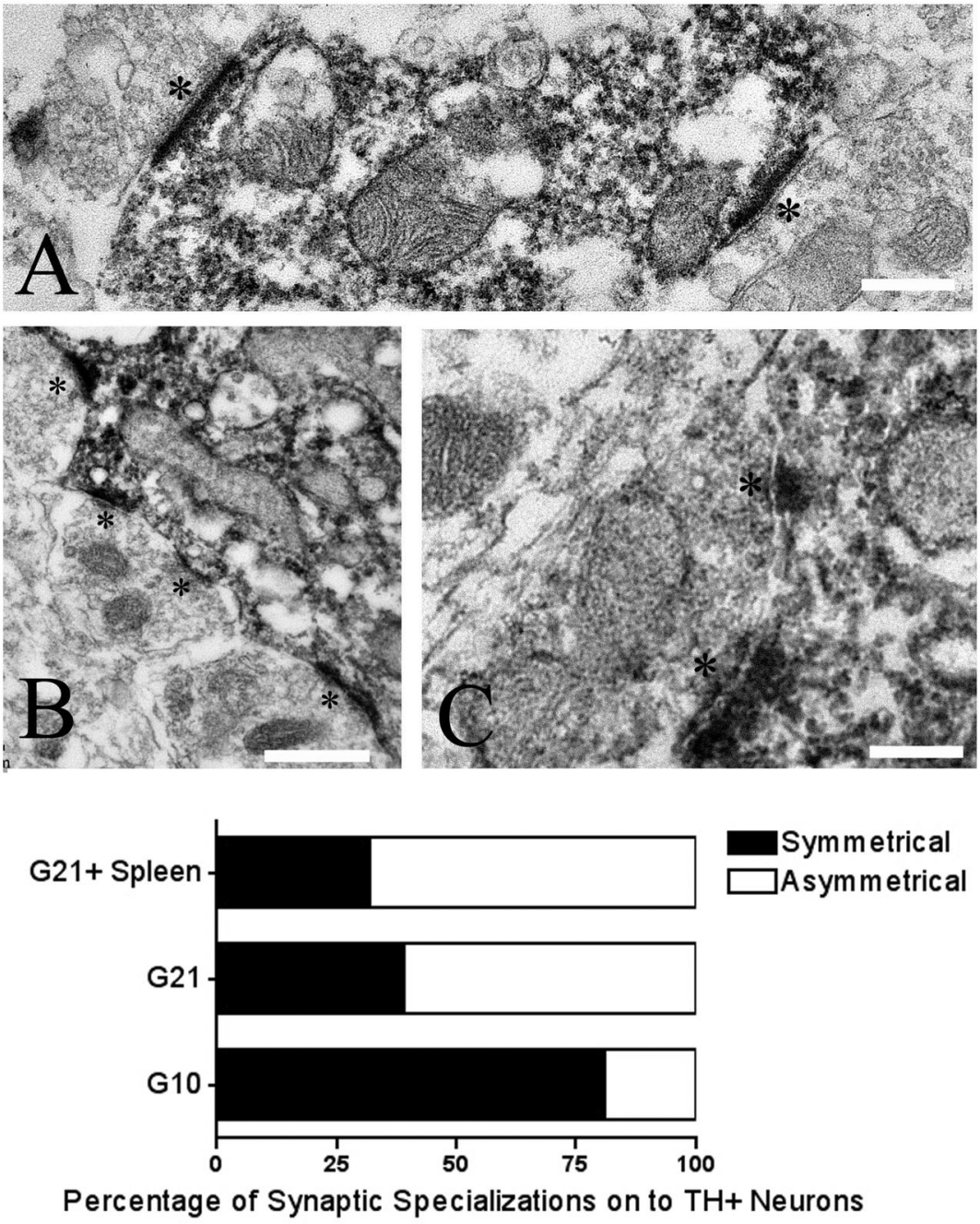

Figure 7. High power electron micrographs illustrating unlabeled synapses (asterisks) onto TH+ dendrites (A, C) and soma (B) in the grafted striatum

Scale bars in A and C= 150nm; scale bar in B= 300nm. The quantitative distribution of the synaptic specializations of these terminals onto TH+ cell bodies and proximal dendrites in the grafted striatum differed significantly between the allografted groups ($p < 0.001$) with a significantly greater percentage of asymmetric synapses seen in G21 and G21 + spleen rats compared to G10 rats (G10 vs. G21: $p < 0.001$, G10 vs. G21 + spleen: $p < 0.001$).

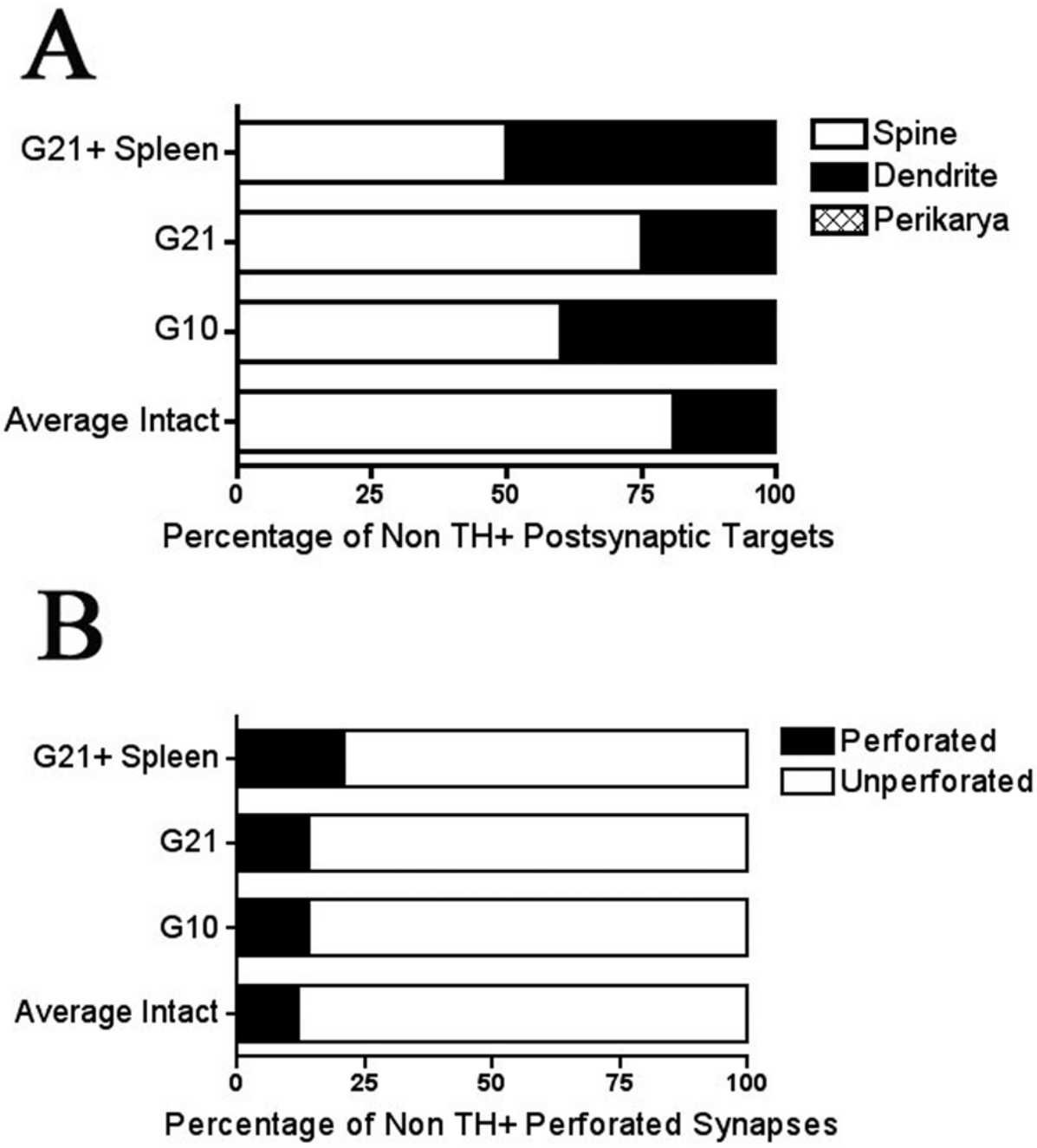

Figure 8. Quantitative distribution of non-TH+ postsynaptic targets (A) and perforation status (B)

(A) In the dopamine-grafted striata, the distribution of postsynaptic targets of non-TH+ synapses differed significantly from their intact hemispheres ($p < 0.001$). Further, dopamine-grafted groups differed from one another ($p = 0.001$), with grafted groups having increased immune activation (G10 and G21 + spleen) showing a significantly greater percentage of inputs onto dendrites rather than spines (G10 vs. G21: $p = 0.035$, G21 + spleen vs. G21: $p < 0.001$). These groups, however, did not differ from one another (G10 vs. G21 + spleen: $p = 0.201$). (B) In the dopamine-grafted striata, the distribution of perforated synapses did not differ significantly from the intact hemisphere in either G10 or G21 rats ($p = 0.25$). However, in grafted rats with increased immune activation there was a significant difference between both

the grafted and intact hemisphere ($p < 0.05$) as well as with G10 ($p<0.05$) and G21 ($p < 0.05$) rats.

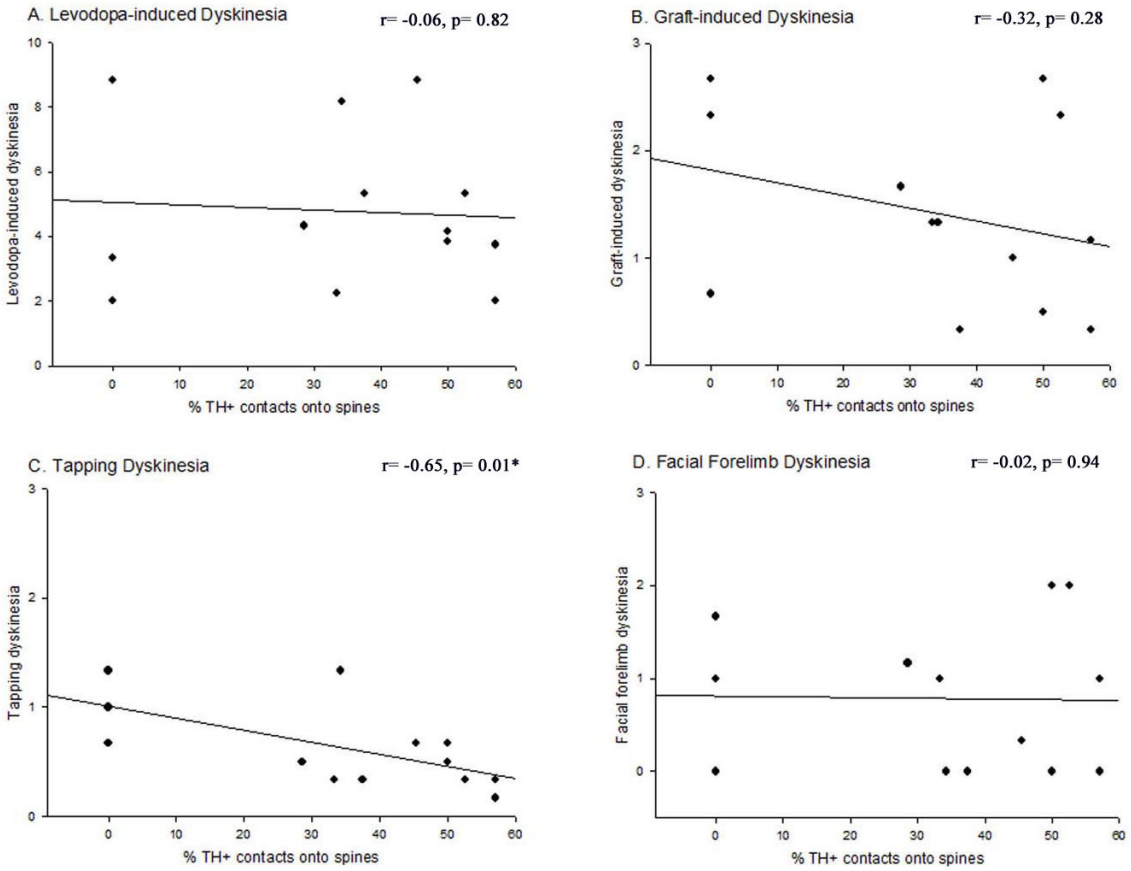

Figure 9. Correlation between the percentage of contacts made by grafted cells onto dendritic spines in the dopamine-depleted striatum and dyskinetic behavioral profiles

The percentage of TH+ contacts onto spines was significantly, negatively correlated with tapping dyskinesias (C; r=−0.65, p=0.005), however, there was no significant correlation of this synapse profile with LIDs (A; p=0.91), total GIDs (B; p=0.31), or facial forelimb dyskinesias alone (D; p=0.78).

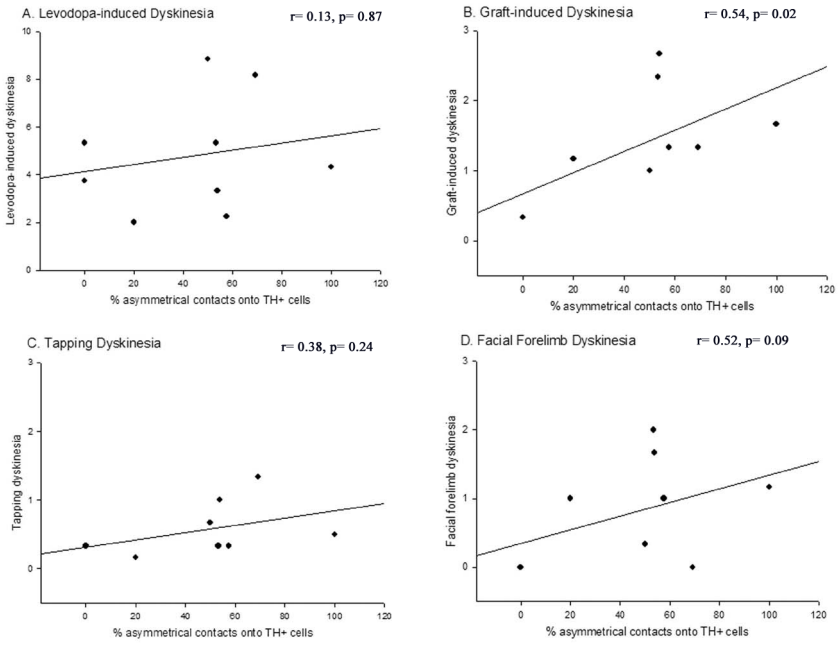

Figure 10. Correlation between the percentage of non-TH+ asymmetric contacts onto grafted cells in the dopamine-depleted striatum and dyskinetic behavioral profiles

The percentage of asymmetric contacts onto TH+ cells was significantly, positively correlated with total GIDs behavior (B; p=0.02), but not with LIDs (A; p=0.87), tapping dyskinesias alone (C; p=0.09), or facial forelimb dyskinesias alone (D; p=0.24).

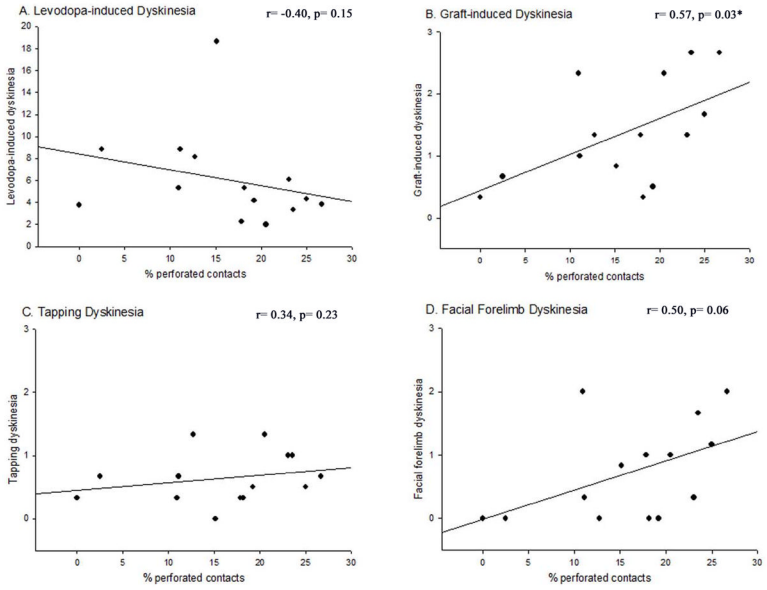

Figure 11. Correlation between the percentage of non-TH+ perforated asymmetric contacts in the dopamine-depleted striatum and dyskinetic behavioral profiles

The percent of perforated asymmetric contacts onto TH+ cells was significantly, positively correlated with total GIDs behavior (B; p=0.03), but not with LIDs (A; p=0.15), tapping dyskinesias alone (C; p=0.23), or facial forelimb dyskinesias alone (D; p=0.06).

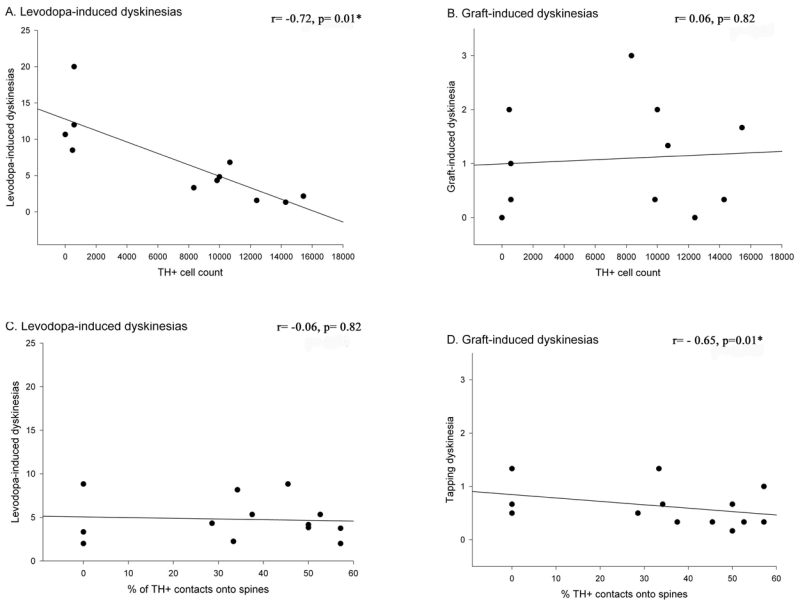

Figure 12. Correlation between the levodopa-induced dyskinesias (A, C) and graft-induced aberrant behaviors (B, D) and TH+ cell counts (A, B) and aberrant synaptology (C, D)

While classic LID-like behaviors correlated positively to the number of surviving TH+ cells in the grafted striatum, they did not correlate with the aberrant synaptic features noted in this study. This is in contrast to GID-like behaviors observed which correlated significantly with aberrant synaptology but not with TH+ cell counts.

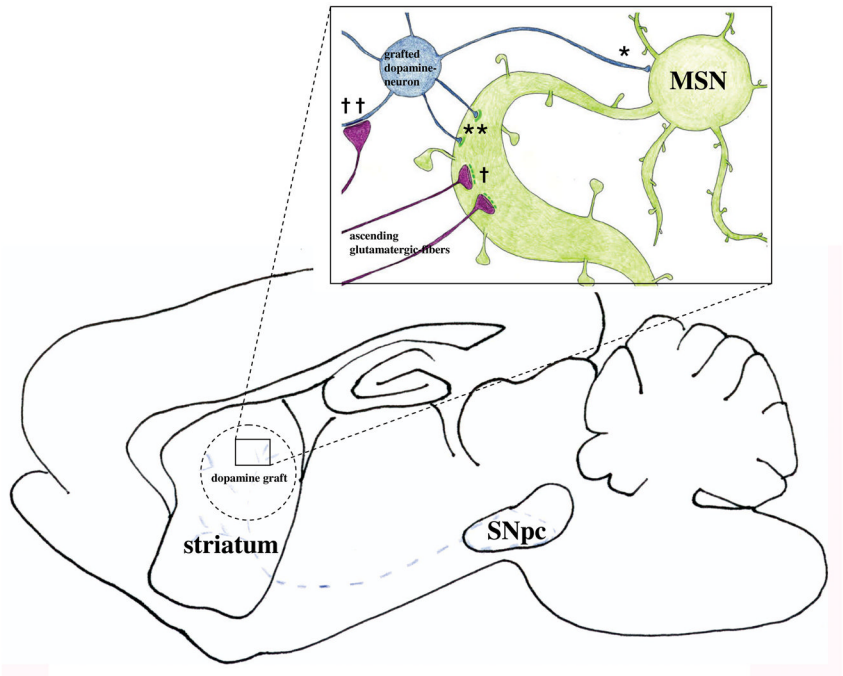

Figure 13. Illustration summarizing the aberrant synaptic features observed in the grafted striatum of rats with elevated immune status and high level dyskinesia

A dopamine graft, in an environment of elevated immune factors, may be a target of aberrant focal activation, creating an excess excitatory drive in the grafted stratium. It is well established that focal stimulation of striatum results in focal output of stereotyped behavior, which is dependent upon which area of striatum is stimulated (Mink et al., 2003; Kelley et al., 1994). The distributions of TH+ axo-dendritic and axo-somatic synapses (*), TH+ asymmetric specializations (**), non-TH+ perforated syanpses (†), and asymmetrical synapses onto TH+ cells (††) were all significantly increased in allografted rats with increased immune activation. These increases in aberrant synaptic features in the allografted striatum, may represent a mechanism by which focal striatal excitation is driving aberrant behaviors following grafting in this study.

Table 1

Summary of the changes in synaptic features observed following grafting and immune challenge, and their correlation with GIDs-like behavior.

Synaptic Features	Grafting	Immune Response	GIDs
TH+ synaptic features (Figure 6)			
• Target Shift	+	+++	correlated
• TH+ Asym	+	+++	not correlated
Input onto grafted DA neurons (Figure 7)			
• Asym Input	−	++	correlated
Non-DA changes (Figure 8)			
• Target shift	+++	+++	not correlated
• Perforations	+	+	correlated